SANDIA REPORT

SAND2008-6185
Unlimited Release
Printed September 2008

Effects of Porosity and Pore Morphology on the Elastic Properties of Unpoled PZT 95/5-2Nb

Stephen T. Montgomery

Prepared by
Sandia National Laboratories
Albuquerque, New Mexico 87185 and Livermore, California 94550

Sandia is a multiprogram laboratory operated by Sandia Corporation,
a Lockheed Martin Company, for the United States Department of Energy's
National Nuclear Security Administration under Contract DE-AC04-94AL85000.

Issued by Sandia National Laboratories, operated for the United States Department of Energy by Sandia Corporation.

Available to DOE and DOE contractors from
U.S. Department of Energy
Office of Scientific and Technical Information
P.O. Box 62
Oak Ridge, TN 37831

Telephone: (865) 576-8401
Facsimile: (865) 576-5728
E-Mail: reports@adonis.osti.gov
Online ordering: http://www.osti.gov/bridge

Available to the public from
U.S. Department of Commerce
National Technical Information Service
5285 Port Royal Rd.
Springfield, VA 22161

Telephone: (800) 553-6847
Facsimile: (703) 605-6900
E-Mail: orders@ntis.fedworld.gov
Online order: http://www.ntis.gov/help/ordermethods.asp?loc=7-4-0#online

SAND2008-6185
Unlimited Release
Printed September 2008

Effects of Porosity and Pore Microstructure on the Elastic Properties of Unpoled PZT 95/5-2Nb

Stephen T. Montgomery
Solid Mechanics Department

Sandia National Laboratories
P.O. Box 5800
Albuquerque, NM 87185-0346

Abstract

Effects of porosity level and pore morphology on the isotropic elastic responses of unpoled porous PZT 95/5-2Nb ferroelectric ceramic are characterized using a simple isotropic elastic response model giving relations between the average stresses and strains of the porous ceramic and the solid matrix surrounding the pores. The model parameters depend on the elastic properties of the solid ceramic material, volume fraction of pores, and two additional material properties that reflect the composition and microstructure of the composite material. Measurements of the effective bulk modulus and shear modulus of the porous ceramic, with corresponding expressions for these quantities from the response model, allow characterization of the additional material properties. It is found that the two material properties reflecting the effect of pore morphology and grain size on the elastic response of unpoled porous PZT 95/5-2Nb ferroelectric ceramics can be expressed in a form that depends explicitly on the porosity level and two parameters dependent solely on the pore morphology and ceramic grain size. Two applications of the model are presented: a simple prediction of the effective bulk modulus and shear modulus for the porous ceramic as a function of porosity for the pore morphologies and grain sizes examined, and a prediction of the effective volume strains, including effects due to the ferroelectric to antiferroelectric phase transformation, for the various ceramics during hydrostatic pressurization.

Acknowledgements

The author would like to thank Joshua Robbins and Timothy Scofield for reviewing this report and providing helpful suggestions for improving the presentation of the material.

Contents

Figures

Figures - continued

Tables

1. Introduction

The ceramic material PZT 95/5-2Nb is a solid solution of lead zirconate and lead titanate having a Zr:Ti ratio of 95:5 and where some of the Zr^{4+} and Ti^{4+} ion sites in the crystal have been replaced, to increase the electrical resistance[1] of the ceramic, with Nb^{5+} by adding 2% niobium during processing. As shown by Fritz and Keck,[2] this material undergoes a ferroelectric (FE) to antiferroelectric (AFE) phase transformation at roughly 300 MPa when hydrostatically compressed. Rapid release of the bound charge, compensating the remanent polarization of the FE phase from electrically poled ceramic by shock compression[3,4] into the AFE phase, provides a controlled release of charge to drive electric loads.

The remanent polarization and fracture toughness of ferroelectric (FE) ceramics[5,6] can be modified by controlling the grain size and porosity. While choice of sintering temperature provides some control over the grain size and porosity of the ceramic, a more precise control of the amount and morphology of the porosity can be achieved by mixing discrete organic pore formers into the ceramic powder casts prior to bisque firing. Tuttle *et al.*[7] have investigated the effect of porosity on the pressure induced FE to AFE phase transformation for two variants of PZT 95/5-2Nb ceramic, having different average grain sizes, fabricated from a common source of chemically prepared PZT 95/5 powder with varying amounts of organic rod-like microcrystalline cellulose (MCC) particles. A decrease in the pressure required to drive the ceramic into the AFE phase was observed as the porosity of the ceramic increased. It was postulated that if the transformation in the ceramic occurred at a specific value of volumetric strain (measured as positive in compression) independent of initial density and roughly equal to 0.4%, as reported by Zeuch *et al.*,[8] the observed decrease in apparent transformation pressure would be consistent with a similar decrease in bulk modulus of the ceramic with increasing porosity. A model to support this conjecture was not presented and it was noted that this mechanism would not account for the observed spread in range of pressure required for the transformation as porosity of the ceramic increased. Similar observations on the effect of increasing porosity in lowering and increasing the range for the apparent pressure needed to produce the FE to AFE phase transformation were reported by Yang *et al.*[9] for ceramic samples of varying porosity fabricated from a common source of chemically prepared PZT 95/5 powder

and varying amounts of spherically shaped polymethyl methacylate (PMMA) particles with diameters ranging from 5 to 40 μm.

Montgomery and Zeuch[10] presented a specific mechanics based microstructural model to account for the effect of porosity on the FE to AFE phase transformation under hydrostatic compression for unpoled PZT 95/5-2Nb ceramic containing spherical voids. The model demonstrated that the local non-uniform stress field in the solid ceramic material surrounding the pores increased with porosity level explaining both the apparent decrease in transformation pressure and, with a fixed the orientation dependent phase transformation condition in the solid ceramic, spreading in the range of pressure across which the transformation occurs.

In this study, the effects of porosity and pore morphology on the elastic response of three types of unpoled porous PZT 95/5-2Nb ceramic are characterized in the context of a specific elastic response model. The three types of ceramic selected for characterization have a common chemical composition but, as described in more detail below, were processed using two different organic pore formers and sintering temperatures to produce samples at various porosity levels with three different microstructures.

First, a model for the elastic response of porous solids is presented in terms of the average stresses and strains of the overall porous material and the solid matrix material surrounding the pores. The elastic response of the porous solid is seen to depend on five parameters: the level of porosity, two elastic moduli of the solid matrix material, and two parameters that characterize the relation between the average strains in the porous ceramic and solid matrix. These last two parameters reflect specific effects of ceramic microstructure such as pore morphology and grain size on the elastic response of the porous ceramic. Relations between the model parameters and effective bulk modulus and effective shear modulus for the ceramic that allow characterization of the model parameters are then described. Two simple methods of estimating the effective bulk modulus and effective shear modulus of porous materials are discussed in the context of the response model used in this study. Details of model development are given in an appendix to this report.

A description of model parameter characterization from experimental measurements, including details of the materials selected for characterization and a methodology for estimating the elastic moduli for the solid matrix material, is given next. Examination of the effects of pore morphology and grain size on the two parameters related to the material microstructure is

described, and it is shown that the three types of ceramic examined in this study can be characterized by four parameters that are independent of porosity level.

As a consistency exercise, the model equations used with the values of material parameters obtained from the characterization are shown to provide reasonable estimates for the measured values for the effective bulk modulus and effective shear modulus of the materials examined. A more complex application is then provided in which the elastic response model, with a simple extension, is shown to provide reasonable predictions for the average volumetric strain of porous ceramic undergoing a FE to AFE phase transformation under hydrostatic pressurization.

2. An Elastic Response Model for Porous Ceramic

Isotropic porous ceramics are often modeled as isotropic linear elastic solids that can be characterized by two effective elastic properties. Implied in this treatment is the assumption that variations in the tractions and displacements applied to these materials occur over a length scale much larger than the characteristic length scale characterizing the pore morphology in the material and that the local fluctuations in stresses and strains within the material average to zero so that well defined macroscopic values for effective stresses and strains exist. However, even with these assumptions, an elastic response model for porous ceramic with a richer structure than is available by just using effective elastic properties to describe the response can be developed, and is useful when it is desirable to explicitly account for porosity, pore morphology effects, and phase transformations in the solid ceramic matrix.

An elastic response model which gives the average stresses and strains in the porous ceramic in terms of explicit porosity measures and the average stresses and strains in the ceramic matrix follows directly from a model developed by Hill[11] (see Appendix A) to describe the equilibrium responses of a discretely reinforced composite material, consisting of perfectly bonded and uniformly distributed inclusions in a solid isotropic elastic matrix, by interpreting the inclusion phase as stress-free void space.

Porous Response Model

Consider a fixed mass of porous ceramic subject to a uniform average strain field. Let ρ define the average density of that mass of porous ceramic and ρ_S denote the average density of the solid ceramic in the matrix defining that mass. The volume of space occupied by this fixed mass of porous ceramic is M/ρ and the volume of space occupied by the solid ceramic of the matrix is M/ρ_S where M the fixed mass under consideration. Commonly used measures for the porosity of the fixed mass of material are the void space volume fraction φ given by

$$\varphi = 1 - \frac{\rho}{\rho_S} \ , \tag{2.1}$$

and the distention ratio α given by

$$\alpha = \frac{\rho_S}{\rho} \ . \tag{2.2}$$

These measures of porosity have the obvious connection $\varphi = (\alpha - 1)/\alpha$.

The following model equations result from the considerations of Hill (see Appendix A) when the inclusions become void space, and are used to represent the elastic response of the porous ceramic:

$$\begin{aligned} \tilde{\sigma}_{ij} &= (1-\varphi)\,\tilde{\sigma}^{S}_{ij} \quad \text{or} \quad \alpha\,\tilde{\sigma}_{ij} = \tilde{\sigma}^{S}_{ij} \\ \tilde{\sigma}^{S}_{ij} &= \left(K_S - \frac{2}{3} G_S \right) \tilde{\varepsilon}^{S}_{kk}\,\delta_{ij} + 2\,G_S\,\tilde{\varepsilon}^{S}_{ij} \\ \tilde{\varepsilon}^{S}_{ij} &= \left(\kappa_S - \frac{2}{3}\gamma_S \right) \tilde{\varepsilon}_{kk}\,\delta_{ij} + 2\,\gamma_S\,\tilde{\varepsilon}_{ij} \end{aligned} \tag{2.3}$$

The average stress and strain tensors in the porous ceramic are represented by the quantities $\tilde{\sigma}_{ij}$ and $\tilde{\varepsilon}_{ij}$ respectively. The average stress and strain tensors in the solid matrix are represented by the quantities $\tilde{\sigma}^{S}_{ij}$ and $\tilde{\varepsilon}^{S}_{ij}$ respectively, while K_S is the bulk modulus and G_S is the shear modulus of the matrix material. Standard tensor notation is used[12] with the indices i and j taking values 1, 2, and 3 corresponding to the three orthogonal directions of a rectangular Cartesian coordinate system. It is worth noting that Carroll and Holt[13] present a derivation of the first of (2.3) that depends on the representative volume of porous material being in static equilibrium.

For a specified average strain state $\tilde{\varepsilon}_{ij}$, the second and third of (2.3) provide the average stress and strain in the ceramic matrix provided values for the material parameters K_S, G_S, κ_S, and γ_S are specified. Presumably, both K_S and G_S are known independently for the material comprising the matrix of the ceramic and are independent of any specific microstructure corresponding to the porosity and pore morphology. However, the two parameters κ_S and γ_S represent a linear transformation between the average macroscopic strain in the porous ceramic and the average strain in the solid matrix and therefore, in some sense, represent an equilibrium structural response characteristic of the microstructure. Consequently, these two parameters reflect the specific microstructure of the porous ceramic and should be expected to depend on the porosity and pore morphology as well as the elastic properties of the solid matrix material. As shown in Appendix A, these two parameters can be determined from measured values for the effective bulk modulus K and effective shear modulus G of the particular porous solid of interest through the relations

$$K = 3(1-\varphi)\ \kappa_S\ K_S \quad \text{and} \quad G = 2(1-\varphi)\ \gamma_S\ G_S\,. \tag{2.4}$$

The average stress in the porous ceramic can be determined from the first of (2.3), at a given value for the void space volume fraction, once the average stress in the solid matrix is determined from the second and third of (2.3).

In many applications, interest is restricted to a single particular porous material, and it suffices to measure effective values for K and G for use in an effective linear elastic material model. However, if deeper insight into the role of microstructural properties such as porosity level and pore morphology are of interest, (2.3) and (2.4) provide an improved framework for investigation at a slight increase in complexity.

Approximations for κ_S and γ_S

An alternate use of the model equations presented above should be mentioned since it suggests functional forms for κ_S and γ_S used in the analysis of data described below. Many times it is desired to estimate the elastic properties of porous materials prior to fabrication or in the absence of means to measure effective elastic properties. The relations (2.3) and (2.4) provide a starting point for efforts to develop model based methodologies to estimate K_S and G_S.

A particularly simple example of an estimate for the effective elastic moduli is provided by assuming the average strain in the porous solid and matrix are identical. This assumption leads to $\kappa_S = 1/3$ and $\gamma_S = 1/2$, and gives the following estimates for the effective moduli:

$$K^m = (1-\varphi)\,K_S \quad \text{and} \quad G^m = (1-\varphi)\ G_S\,. \tag{2.5}$$

The superscript "m" indicates that this result is identical to a prediction obtained using the rule of mixtures.

A more sophisticated estimate for the effective moduli is provided for dilute concentrations of spherical pores in the ceramic matrix and the change in pore configuration is included in the approximation. Eshelby[14] considered the elastic response of an isolated inclusion, in the shape of an ellipsoid, embedded in a linear isotropic elastic solid whose shape far from the inclusion is determined by a uniform strain field, and showed that the strain in the inclusion must be uniform and linearly dependent on the far field strain in the surrounding material. In particular, the deformed configuration of an initially spherical void can be determined from a uniform strain ε_{ij}^V that depends on the far field strain ε_{ij} according to

$$\varepsilon_{ij}^{V} = \frac{1}{3}(a-b)\,\varepsilon_{ij}\,\delta_{ij} + b\,\varepsilon_{ij} \tag{2.6}$$

where *a* and *b* are parameters that depend on the elastic properties of the surrounding elastic material.

If the volume fraction of voids is small, then (2.6) may be assumed to represent a linear transformation between the average strain field characterizing the configuration of the voids and the average strain field of the solid matrix, giving

$$\tilde{\varepsilon}_{ij}^{V} = \frac{1}{3}(a-b)\,\tilde{\varepsilon}_{ij}^{S}\,\delta_{ij} + b\,\tilde{\varepsilon}_{ij}^{S} \tag{2.7}$$

with

$$a = \frac{3K_S + 4G_S}{4G_S} \quad \text{and} \quad b = \frac{15(1-\nu_S)}{(7-5\nu_S)} = \frac{5(3K_S + 4G_S)}{(9K_S + 8G_S)} \tag{2.8}$$

where ν_S is Poisson's ratio for the solid ceramic matrix. Using (2.7) and the second of (A.2) [see Appendix A] gives

$$\tilde{\varepsilon}_{ij} = (1-\varphi)\,\tilde{\varepsilon}_{ij}^{S} + \varphi\,\tilde{\varepsilon}_{ij}^{V} = \left\{\frac{1}{3}(a-b)\varphi\right\}\tilde{\varepsilon}_{kk}^{S}\,\delta_{ij} + \left\{1+(b-1)\varphi\right\}\tilde{\varepsilon}_{ij}^{S}\,. \tag{2.9}$$

The third of (2.3) and (2.9) are compatible when

$$3\kappa_S = \frac{1}{\left[1+(a-1)\varphi\right]} \quad \text{and} \quad 2\gamma_s = \frac{1}{\left[1+(b-1)\varphi\right]}\,. \tag{2.10}$$

Substituting these expressions for κ_S and γ_S into (2.4) give the following estimates for the effective moduli

$$K^{D} = \frac{(1-\varphi)K_S}{\left[1+(a-1)\varphi\right]} \quad \text{and} \quad G^{D} = \frac{(1-\varphi)G_S}{\left[1+(b-1)\varphi\right]}\,. \tag{2.11}$$

The superscript "D" indicates these estimates were formed assuming a dilute suspension of voids in the solid matrix. Algebraic manipulation of (2.11) recovers the following approximate expressions for the effective bulk modulus and shear modulus for a porous solid containing different sized spherical pores derived in a different fashion by MacKenzie[15]

$$\frac{1}{K} = \frac{\alpha}{K_S} + \frac{3(\alpha-1)}{4G_S} + O(\varphi^3) \quad \text{and} \quad \frac{(G_S-G)}{G_S} = \frac{5(3G_S+4K_S)}{(8G_S+9K_S)}\,\frac{(\alpha-1)}{\alpha} + O(\varphi^2)\,. \tag{2.12}$$

3. Characterization of Three Types of Porous PZT 95/5-2Nb Ceramic

The porous ceramic model described above is now characterized for three types of unpoled porous PZT 95/5-2Nb ceramic. These porous ceramic materials were selected because they were fabricated under well controlled processing conditions from common lots of PZT powder with the chemical composition,[7,9] $Pb_{0.996}(Zr_{0.953}Ti_{0.047})Nb_{0.018}O_3$, and varying amounts of added organic pore former. Compositions[9], denoted P1350, were fabricated at three levels of porosity, all less than 15%, by adding varying amounts of the PMMA spheres ranging in diameter from 40 to 120 μm to the ceramic material and firing at 1350°C. Compositions[7], denoted M1345, having a nominal grain size of 15 μm were fabricated at four levels of porosity, each less than 15%, by adding varying amounts of the MCC rods ranging in size from 5 to 70 μm to the ceramic material and firing at 1345°C. Compositions[7], denoted M1275, having a nominal grain size of 10 μm were fabricated at three levels of porosity, again all less than 15%, by adding varying amounts MCC rods to the ceramic material and firing at 1275°C. The composition types M1275 and M1345 provide a means to examine effects of grain size on elastic response for similar pore morphologies since the same organic pore was used and only sintering temperature was varied. The composition types M1345 and P1350 provide a means to examine the effect of pore morphology on the elastic properties for porous ceramics made using different types of organic pore formers yet having nearly the same grain size due to the similarity of the sintering temperature used in fabrication.

Effective Property Measurements for Unpoled Porous PZT 95/5-2Nb

Densities of the porous ceramic samples were determined using the Achimedes technique while longitudinal and shear wave speeds were measured across opposing parallel faces of samples using pulse-echo or time-of-flight techniques with effective values for elastic moduli calculated assuming an elastically isotropic unpoled ceramic.[9] The values for the effective density, bulk modulus, and shear modulus for samples of the unpoled porous PZT 95/5-2Nb specimens with less than 15% void volume fraction are listed in Table 1. The values in Table 1 for the effective bulk modulus of M1345 and M1275 are as reported[7] while corresponding effective shear modulus was derived from the effective bulk modulus and the average of values for Young's modulus. Only samples of M1345 and M1275 actually containing the MMC pore former are listed since the processing history for two higher density samples reported, without

added pore former, must necessarily be different. The values for the effective bulk modulus and effective shear modulus for the samples fabricated using the PMMA pore former were calculated from averages of reported stiffness values (see Table 2 of Yang *et al.* [9]). The values of void volume fraction and distention ratio for each sample were calculated from (2.1) and (2.2) assuming the solid matrix has theoretical density of 8.03 g/cm^3.

TABLE 1. Properties for unpoled porous PZT95/5-2Nb ceramic samples.

Sample Type	Density (kg/m^3)	φ	α	K (GPa)	G (GPa)
P1350	7366	0.080	1.087	68.3	47.9
P1350	7145	0.108	1.121	63.5	44.7
P1350	6940	0.134	1.155	59.1	41.9
M1345	7714	0.037	1.038	72.8	51.7
M1345	7650	0.045	1.047	70.5	49.5
M1345	7393	0.077	1.083	63.4	45.9
M1345	7121	0.111	1.125	53.6	39.7
M1275	7626	0.048	1.050	71.0	50.4
M1275	7393	0.077	1.083	64.0	46.6
M1275	7121	0.111	1.125	55.5	41.7

Model Parameter Characterization for Unpoled Porous PZT 95/5-2Nb Samples

In addition to the void volume fraction, four additional material constants are needed to characterize the model equations. For many porous materials, such as foamed metals, the bulk modulus and shear modulus of the solid matrix material are known from independent measurements on the solid, and consequently only the parameters κ_S and γ_S need to be determined. However, for the unpoled porous PZT 95/5-2Nb ceramic the bulk modulus and shear modulus of the solid ceramic matrix are not known because it is not easy to fabricate large samples without porosity due to the conditions used in sintering the material. Fortunately there are enough measurements at different levels of porosity on the three types of unpoled porous PZT 95/5-2Nb ceramic to establish reliable estimates for the bulk modulus and shear modulus of

the solid matrix using the expressions for the effective moduli and extrapolation to a vanishing level of porosity. Note that (2.4) can be written

$$\frac{1}{K} = \frac{1}{3\kappa_S K_S}\alpha \quad \text{and} \quad \frac{1}{G} = \frac{1}{2\gamma_S G_S}\alpha . \tag{3.1}$$

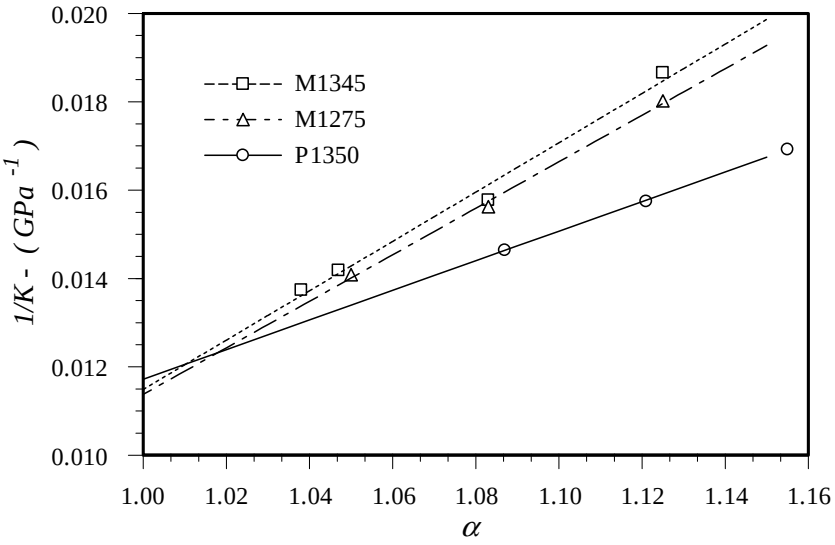

Fig. 1 Variation of $1/K$ with distention ratio for the three PZT 95/5-2Nb ceramic types. Linear least squares fits to measure values (symbols) for each type of ceramic are indicated by the lines.

Figures 1 and 2 show values for the inverses of the effective bulk modulus and effective shear modulus for each type of unpoled porous PZT 95/5-2Nb ceramic at the corresponding distention ratio with linear least square fits to the data that appear to converge to nearly common values as the level of porosity vanishes ($\alpha \to 1$). Since $\kappa_S \to 1/3$ and $\gamma_S \to 1/2$ as $\alpha \to 1$, estimates of K_S and G_S follow directly from the linear least squares fits at $\alpha = 1$. Averaging the values for each type of porous ceramic gives a solid bulk modulus of 86.7 GPa and a shear modulus of 58.9 GPa for solid PZT 95/5-2Nb ceramic. Since the individual values for each type of porous ceramic are within 2% of the average for the solid bulk modulus and 0.5% of the average for the solid shear modulus, it is reasonable to use these values for solid PZT 95/5-2Nb ceramic independent of the specific type of pore former and processing history used to fabricate the ceramic.

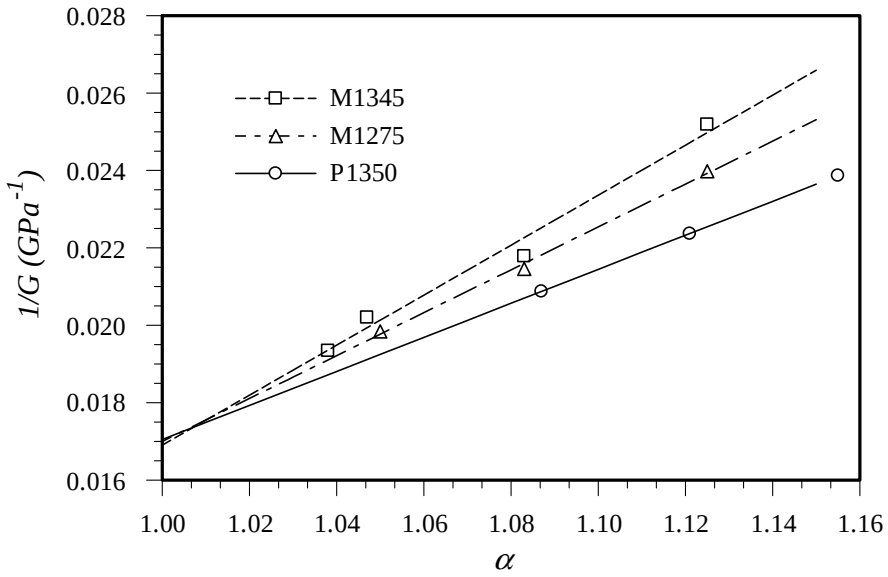

Fig. 2 Variation of $1/G$ with distention ratio for the three PZT 95/5-2Nb ceramic types. Linear least squares fits to measure values (symbols) for each type of ceramic are indicated by the lines.

The values of κ_S and γ_S needed to complete the characterization the elastic response model given by (2.3) can be calculated directly from (2.4) for each sample of porous ceramic examined and are listed in Table 2.

TABLE 2. Values of κ_S and γ_S for unpoled porous PZT95/5-2Nb samples.

Sample	Density (kg/m^3)	φ	α	κ_S	γ_S
P1350	7366	0.080	1.087	0.285	0.442
P1350	7145	0.108	1.121	0.274	0.425
P1350	6940	0.134	1.155	0.262	0.411
M1345	7714	0.037	1.038	0.291	0.456
M1345	7650	0.045	1.047	0.284	0.440
M1345	7393	0.077	1.083	0.264	0.422
M1345	7121	0.111	1.125	0.232	0.379
M1275	7626	0.048	1.050	0.287	0.449
M1275	7393	0.077	1.083	0.267	0.428
M1275	7121	0.111	1.125	0.240	0.398

Effects of Porosity, Pore Morphology, and Grain Size on Model Parameters

The values for φ, κ_S, and γ_S, listed in Table 2, with the elastic properties ($K_S \approx 86.7\,\text{GPa}$ and $G_S \approx 58.9\,\text{GPa}$) characterizing the solid matrix provide the parameters needed to use (2.3) in describing the elastic response of the samples examined. It is evident that the specifics of microstructure (pore morphology and grain size) for these porous ceramics are reflected in the two parameters κ_S and γ_S. Effects on the parameters κ_S and γ_S due to pore morphology, grain size, and porosity level can be examined.

Recall that the dilute suspension approximation for these parameters given by (2.10), depended explicitly on the pore volume fraction and two constants that were determined from the elastic properties of the solid matrix and the spherical geometry assumed for the pores. Using (2.10) as a guide, we assume that κ_S and γ_S can be written in the form

$$\frac{1}{3\,\kappa_S} - 1 = A\,\varphi \quad \text{and} \quad \frac{1}{2\,\gamma_S} - 1 = B\,\varphi \ . \tag{3.2}$$

Note that setting $A = a - 1$ and $B = b - 1$ in (3.2) recovers (2.10). Using the data in Table 2 to form a linear least squares fit, constrained to pass through $\kappa_S = 1/3$ and $\gamma_S = 1/2$ when $\varphi = 0$, provides the values for *A* and *B* shown in Table 3 for each of the three types of porous unpoled PZT 95/5-2Nb.

TABLE 3. Model parameters for three types of porous PZT 95/5-2Nb.

Material Type	K_S (GPa)	G_S (GPa)	A	B
P1350	86.7	58.9	2.04	1.63
M1345	86.7	58.9	3.78	2.74
M1275	86.7	58.9	3.41	2.28

Figures 3 and 4 show the least square fits of the functional form (3.2) to the data listed in Table 3. As seen in Figures 3 and 4, reasonable fits to the experimental data can be achieved with constant values for *A* and *B*. Consequently, to a good approximation, these parameters can be regarded as independent of porosity and primarily reflect the effect of pore former type and sintering temperature. It is evident that ceramic material fabricated with the MCC pore former is characterized by larger values of *A* and *B* than ceramic material fabricated using the PMMA pore former, and that while the values of *A* and *B* are similar for the two materials fabricated using the MCC pore former, there is a discernable effect on the values of these parameters due to sintering temperature, with the values of both parameters being larger for the material sintered at 1345 °C which produces a somewhat larger average grain size.

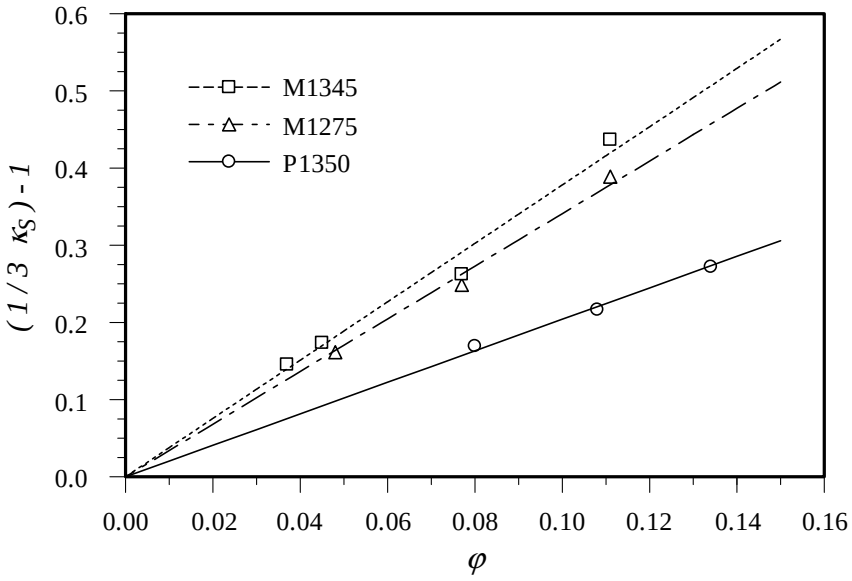

Fig. 3 Linear least squares fits to measured data for the three types of porous PZT 95/5-2Nb examined. Values of A for each type of ceramic are given by the slopes of the least square fits.

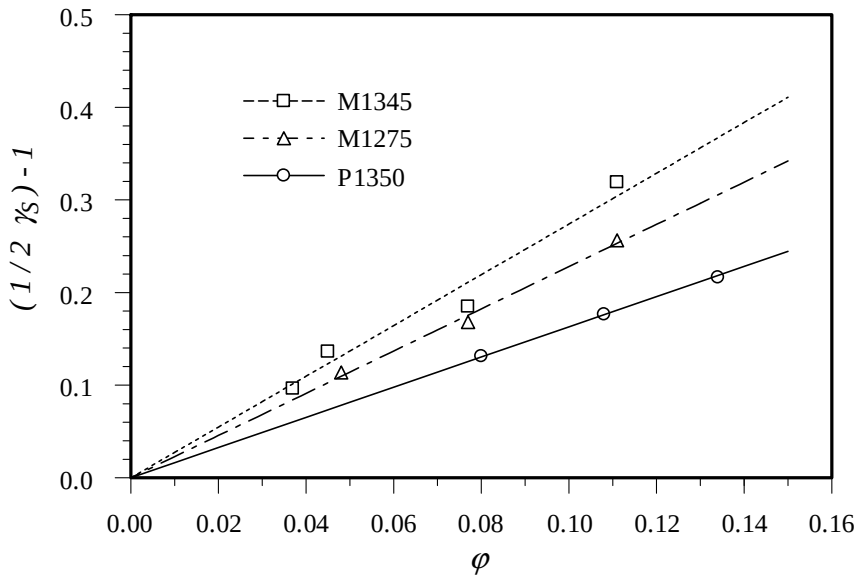

Fig. 4 Linear least squares fits to measured data for the three types of porous PZT 95/5-2Nb examined. Values of B for each type of ceramic are given by the slopes of the least square fits.

4. Response Model Applications

Linear elastic responses for three types of unpoled porous PZT 95/5-2Nb ceramic have been characterized for void volume fractions $\varphi \le 0.14$ using the following equations:

$$\begin{aligned}
\tilde{\sigma}_{ij} &= (1-\varphi)\,\tilde{\sigma}^{S}_{ij} \\
\tilde{\sigma}^{S}_{ij} &= \left(K_S - \frac{2}{3} G_S \right) \tilde{\varepsilon}^{S}_{kk}\, \delta_{ij} + 2 G_S\, \tilde{\varepsilon}^{S}_{ij} \\
\tilde{\varepsilon}^{S}_{ij} &= \left(\kappa_S - \frac{2}{3} \gamma_S \right) \tilde{\varepsilon}_{kk}\, \delta_{ij} + 2 \gamma_S\, \tilde{\varepsilon}_{ij} \\
\kappa_S &= \frac{1}{3\left[1 + A\,\varphi\right]} \\
\gamma_S &= \frac{1}{2\left[1 + B\,\varphi\right]}
\end{aligned} \tag{4.1}$$

These equations depend explicitly on void volume fraction and with the four additional parameters K_S, G_S, A, and B (listed in Table 3) describe the linear elastic response of the three types of unpoled porous PZT 95/5-2Nb ceramics examined in this report. The elastic moduli, K_S and G_S, are common to all three types of porous ceramic. The remaining two parameters A and B reflect microstructural differences in the ceramic produced during fabrication due to the use of one of two types of organic pore former and a change in grain size reflecting the sintering temperature. Two applications using (4.1) are presented below.

Effective Elastic Moduli

Substituting the last two of (4.1) into (2.4) gives the following predictions for the effective bulk modulus and effective shear modulus of the porous ceramic at various void volume fractions:

$$K = \frac{(1-\varphi)\,K_S}{\left[1 + A\,\varphi\right]} \quad \text{and} \quad G = \frac{(1-\varphi)\,G_S}{\left[1 + B\,\varphi\right]}\,. \tag{4.2}$$

The continuous curves in Figures 5 and 6 illustrate the variations of effective bulk modulus and effective shear modulus with void volume fraction across the range $0 \le \varphi \le 0.15$ predicted using (4.2) and the model parameters in Table 3. It is evident that the effective moduli decrease with increasing void volume fraction for all three ceramic formulations.

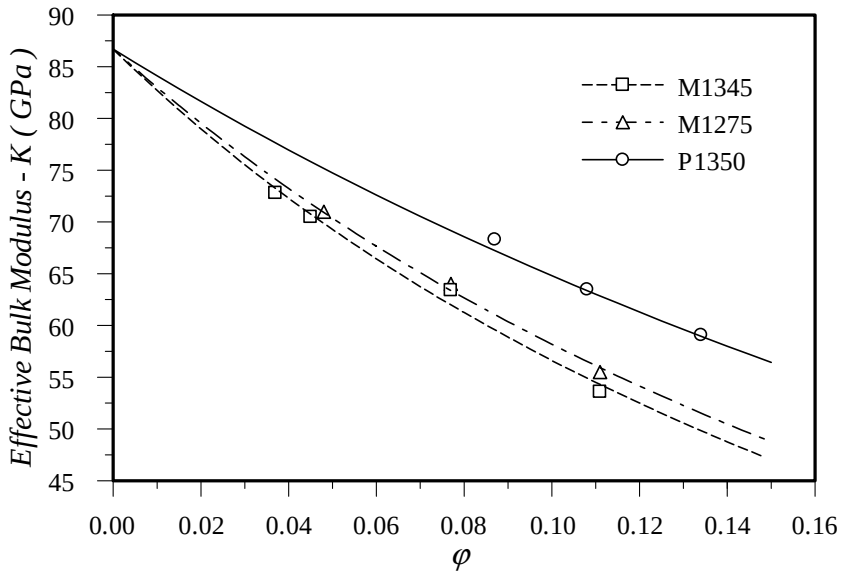

Fig. 5 Effect of void volume fraction on the effective bulk modulus for porous PZT 95/5-2Nb ceramic. The lines result from using (4.2) with parameters from Table 3 while measured values are indicated by the symbols.

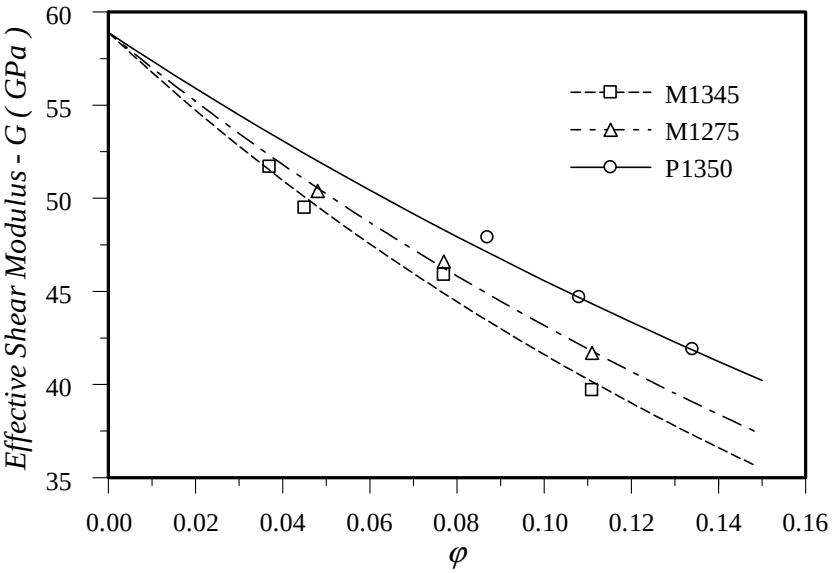

Fig. 6 Effect of void volume fraction on the effective shear modulus for porous PZT 95/5-2Nb ceramic. The lines result from using (4.2) with parameters from Table 3 while measured values are indicated by the symbols.

It is also seen that the type of pore former used to fabricate the ceramic has the most significant effect on the effective moduli. Figures 5 and 6 show that for a common void volume fraction, the ceramic fabricated using the spherical PMMA pore formers is stiffer than the two ceramics fabricated using the MCC pore former. The effect of grain size on the elastic moduli produces a less significant difference in material responses as illustrated by the effective moduli curves for the ceramics M1345 and M1275, both fabricated using the MCC pore former, but sintered at different temperatures to produce similar materials with different average grain sizes. These results indicate that PZT 95/5-2Nb is more compliant as the grain size increases.

Hydrostatic Compression: Ferroelectric to Antiferroelectric Phase Transformation

Zeuch *et al.*[16] have examined the mechanical response of porous FE ceramics undergoing a transformation from the FE to AFE phase under hydrostatic compression and Figure 7 illustrates a typical volumetric strain response as the applied pressure on porous PZT 95/5-2Nb is increased at a constant rate. As can be seen, the volumetric strain, which is reckoned as positive in compression, shows an initial increase proportional to pressure until the onset of the FE to AFE phase transformation. Since the specific volume of the AFE phase is smaller than the specific

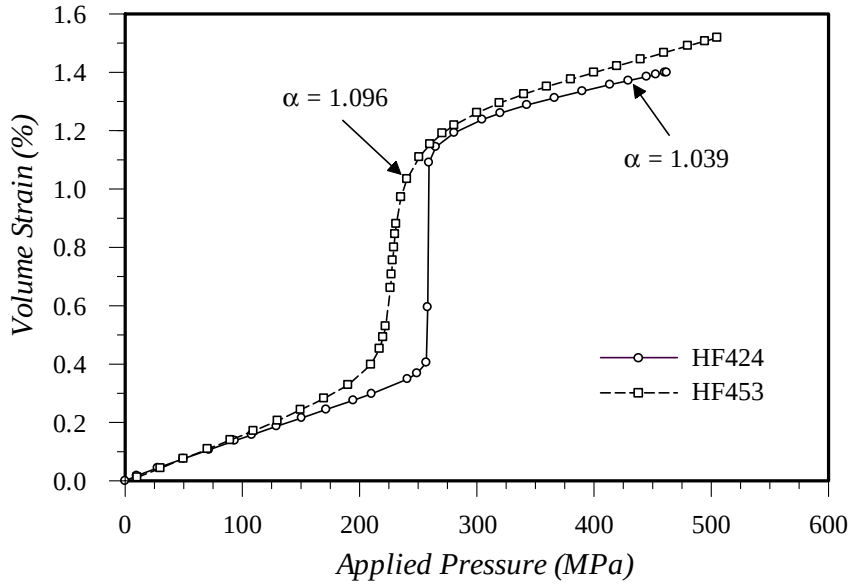

Fig. 7 Average volume strain as applied pressure is increased for two ceramics (HF424 and HF453) having different porosities.

volume of the FE phase, the volume strain accumulates very rapidly with pressure through the phase transformation. As the pressure continues to increase, the phase transformation nears completion and the volume strain again shows an increase proportional to the increase in applied pressure. The response curves shown in Figure 7 were obtained for a PZT 95/5 composition (HF424) fabricated without any organic pore former or added niobium and a PZT 95/5-2Nb composition fabricated with a spherical PMMA pore former. In the following, the model developed above is used to examine the response of porous ceramic whose solid matrix undergoes an FE to AFE phase transformation under hydrostatic compression.

Since it is assumed that the average stress and strain tensors describing the porous ceramic under an applied hydrostatic pressure loading are well represented as hydrostatic, the off-diagonal components of the stress and strain tensors vanish and all diagonal components are equal. We therefore have:

$$\begin{aligned} &\tilde{\sigma}_{12} = \tilde{\sigma}_{23} = \tilde{\sigma}_{13} = 0 \qquad && \tilde{\sigma}_{11} = \tilde{\sigma}_{22} = \tilde{\sigma}_{33} = -P \\ &\tilde{\varepsilon}_{12} = \tilde{\varepsilon}_{23} = \tilde{\varepsilon}_{13} = 0 \qquad && \tilde{\varepsilon}_{11} = \tilde{\varepsilon}_{22} = \tilde{\varepsilon}_{33} = -e_V/3 \\ &\tilde{\sigma}^S_{12} = \tilde{\sigma}^S_{23} = \tilde{\sigma}^S_{13} = 0 \qquad && \tilde{\sigma}^S_{11} = \tilde{\sigma}^S_{22} = \tilde{\sigma}^S_{33} = -P^S \\ &\varepsilon^S_{12} = \varepsilon^S_{23} = \varepsilon^S_{13} = 0 \qquad && \varepsilon^S_{11} = \varepsilon^S_{22} = \varepsilon^S_{33} = -e^S_V/3 \end{aligned} \tag{4.3}$$

Here P is the pressure in the porous ceramic and is equal to the applied pressure on the porous ceramic, P^S is the pressure in the solid matrix, e_V is the magnitude of the volumetric strain in the porous ceramic, and e_V^S is the magnitude of the volumetric strain in the solid matrix. Substitution of (4.3) into (4.1), and replacing φ with α, gives

$$\begin{aligned} &P^S = \alpha P \\ &P^S = K_S\, e_V^S \\ &e_V = \left[1 + A\left(\alpha - 1\right)/\alpha\right] e_V^S . \end{aligned} \tag{4.4}$$

It is reasonable to expect that the phase transformation between the FE and AFE phases depends only on conditions within of the solid matrix of the porous ceramic. A common assumption is that the phase transformation occurs when the average pressure in the solid matrix reaches a critical fixed value, P_T^S, called the hydrostatic transformation pressure. As long as the average pressure in the solid matrix is less than P_T^S the material will remain in the FE phase, but when the average pressure in the solid matrix exceeds the transformation pressure, the material

transforms to the AFE phase. If we set $P^S = P_T^S$ in the first of (4.4), the following expression for the critical applied pressure, P_T, at which a porous ceramic transforms into the AFE phase is obtained

$$P_T = (1-\varphi)\, P_T^S . \tag{4.5}$$

The observation that the apparent transformation pressure for porous PZT 95/5-2Nb ceramics decreases as the porosity of the ceramics increase is clearly consistent with an assumption that the phase transformation occurs at a fixed value for the pressure in the solid matrix. It is not so clear that an effect due to microstructure should be absent in (4.5). The second and third of (4.4) can be used to calculate the average volume strain at the onset of the phase transformation and yield

$$e_{TV} = [1 + A\,\varphi]\, e_{TV}^S . \tag{4.6}$$

Here e_{TV}^S is the volume strain in solid FE ceramic at the onset of the phase transformation and is given by

$$e_{TV}^S = P_T^S / K_S \tag{4.7}$$

and it is also assumed that the solid matrix is entirely FE when $P_S < P_T^S$. The result provided by (4.6) indicates that the average volume strain of the porous ceramic at the onset of the FE to AFE phase transformation will increase as the porosity increases. Figure 8 illustrates the behavior of the effective critical applied pressure and corresponding average volume strain for porous ceramic at the onset of the phase transition with varying levels porosity.

The estimates for the apparent pressure and average volume strain at the onset of the FE to AFE phase transformation were obtained assuming the onset of the transformation could be specified using a critical value for the average pressure in the solid matrix. Zeuch *et al.*[16] investigated the response of unpoled ceramic to non-hydrostatic stress and observed that the assumption that a critical value of the mean stress for the onset of the phase transformation did not hold in general, and they proposed that the onset of the FE to AFE phase transformation must depend on the complete stress state and the crystallographic orientations of the FE domains in the ceramic grains. Montgomery and Zeuch[10] proposed the specific condition that a

transformation of a FE domain to the AFE phase will occur when the normal stress (reckoned as positive in compression) on a plane perpendicular to the direction of the spontaneous polarization, σ_{FD} in the FE domain exceeds a critical value, P_T^S. This condition reverts to a critical value of pressure for hydrostatic loading on the ceramic, and also explains transformation behavior observed during non-hydrostatic loading.[16] In order to apply this more general transformation condition in the analysis of unpoled porous PZT 95/5-2Nb ceramic response, some generalization of the elastic response model presented above and a means of estimating stress variations in the vicinity of a pore are now developed.

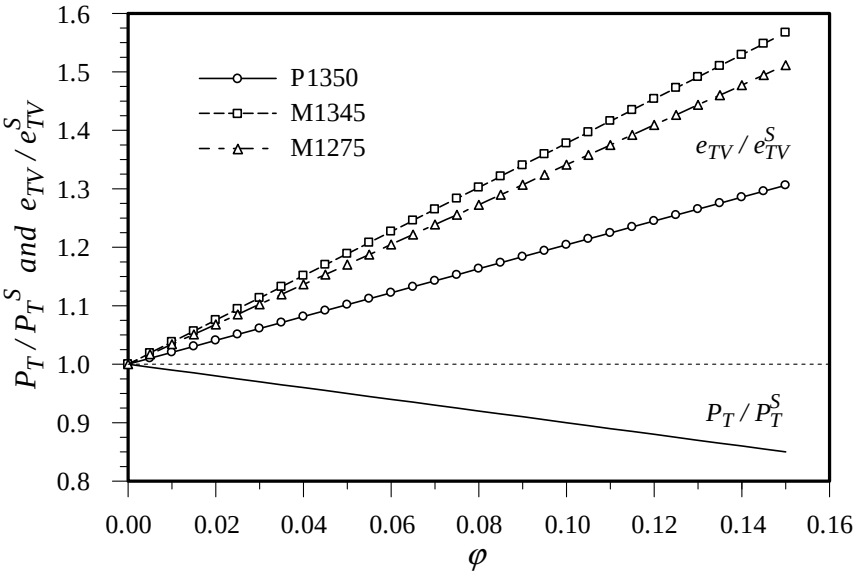

Fig. 8 Model predictions for the pressure and average volume strain at the start of the FE to AFE phase transformation for porous PZT 95/5-2Nb ceramics.

It is assumed that the solid matrix is a mixture of the FE and AFE phases in pressure equilibrium. It is convenient to work with the average specific volume of the solid matrix v_S which is simply the inverse of the average density, *i.e.*,

$$v_S = 1/\rho_S \, . \tag{4.8}$$

Since the solid matrix is a mixture of the FE and AFE phases, (4.8) can be written

$$v_S = F \, v_F + (1-F) \, v_A \tag{4.9}$$

where υ_F and υ_A are the average specific volumes of the FE and AFE phases and F is the mass fraction of the solid matrix in the FE phase. The average specific volumes υ_{0F} and υ_{0A} are associated with pressure free states for the FE and AFE phases. The average pressures in the FE and AFE phases are assumed to be linear in average volume strain, *i.e.*,

$$P_S^F = K_F\, e_V^F \quad \text{and} \quad P_S^A = K_A\, e_V^A \tag{4.10}$$

where K represents the bulk modulus, P_S represents the pressure in the solid components of the mixture and the superscript or subscript "F" and "A" denote the quantity is associated with the FE or AFE phase. The linear elastic volume strains in the FE and AFE phase are[12]

$$e_V^F = 1-\left(\upsilon_F/\upsilon_{0F}\right) \quad \text{and} \quad e_V^A = 1-\left(\upsilon_A/\upsilon_{0A}\right). \tag{4.11}$$

Since pressure equilibrium between the FE and AFE phases implies

$$P_S^F = P_S^A = P^S, \tag{4.12}$$

the relations (4.9), (4.10), and (4.11) may be combined to give the following replacement for the second of (4.4):

$$e_V^S = 1-\left(\frac{\upsilon_S}{\upsilon_{0F}}\right) = \left[1-\left(\frac{\upsilon_{0A}}{\upsilon_{0F}}\right)\right](1-F)+\left[F+\left(\frac{\upsilon_{0A}}{\upsilon_{0F}}\right)\left(\frac{K_F}{K_A}\right)(1-F)\right]\left(\frac{P^S}{K_F}\right). \tag{4.13}$$

In order to use (4.13), a means of calculating F during the loading is required. Earlier it was assumed that the transformation occurs when the pressures in the solid matrix reaches a fixed value, P_T^S, called the hydrostatic transformation pressure. As long as the pressure in the solid matrix is less than the hydrostatic transformation pressure the material remains in the FE phase and $F=1$. However, when the pressure in the solid matrix exceeds the transformation pressure the solid matrix transforms into the AFE phase and $F=0$. The addition of (4.13) into the model allows calculation of the average volume strain as the material transforms into the AFE phase. However, the observed spreading of the transformation across a range of pressure is still not predicted.

The more general phase transformation condition described above is considered next. The calculation of F for an applied stress loading will depend on the stress fluctuations and FE domain orientation distributions in the ceramic grains. Currently, there is no well defined computational or experimental methodology available to determine the dependence of F on the

applied pressure for complex ceramic microstructures. Simulations may provide reasonably accurate calculations for the FE mass fraction provided appropriate representations of ceramic microstructure are available, but there currently appears to be no tested computational methodology. Alternately, it may be possible to find a reasonable representation for F by using the first and third of (4.4) in conjunction with (4.13) and well defined experiments that include carefully selected unload-reload cycles during hydrostatic pressure loading.

Montgomery and Zeuch[10] demonstrated an approximate method to estimate the FE mass fraction using the normal stress based transformation condition and a micromechanical model to represent the local stress variations in the vicinity of a void. The stress equilibrium for a hollow sphere loaded on the outer surface by an applied hydrostatic pressure was selected to represent the non-uniform stress distribution in the vicinity of a spherical void. The inner and outer radii of the sphere can be selected to give a desired distention ratio. The solid portion of the sphere was assumed to be in the FE phase with directions of spontaneous polarization for the FE domains distributed uniformly in space. By using the normal stress based transformation condition and the non-uniform stress state in the sphere wall, the mass fraction at any point in the wall was calculated as a function of the applied pressure. Integration of the mass fraction across the sphere wall then yielded the following analytic expression (where the change of variable $W = P_T^S \big/ (\alpha P)$ is used to simplify the expression) for the FE mass fraction of the hollow sphere:

$$F = \begin{cases} 1 & , \quad W \geq \dfrac{3}{2} \\ 1 - \dfrac{(\alpha - 1)}{(W-1)} \left[1 - \dfrac{2W}{3} \right]^{3/2} & , \quad \dfrac{3}{2} - \dfrac{1}{2\alpha} \leq W \leq \dfrac{3}{2} \\ 1 - \dfrac{(\alpha - 1)}{(W-1)} \left[\left(\dfrac{1}{3} - \dfrac{2(W-1)}{3} \right)^{3/2} - \left(\dfrac{1}{3} - \dfrac{2\alpha(W-1)}{3(\alpha-1)} \right)^{3/2} \right] & , \quad \dfrac{1}{\alpha} \leq W \leq \dfrac{3}{2} - \dfrac{1}{2\alpha} \\ (1-\alpha) - \dfrac{(\alpha - 1)}{(W-1)} \left[1 - \dfrac{2W}{3} \right]^{3/2} & , \quad 0 \leq W \leq \dfrac{1}{\alpha} \end{cases} \tag{4.14}$$

Lacking a better estimate for F, we use (4.14) and the first of (4.4) to calculate the average volume strain in the solid matrix surrounding pores. Then, if we further assume the interaction between the average volume strain in the solid matrix and average volume strain of porous ceramic is not changed due to the phase transformation, the average volume strain of the porous

ceramic can be estimated using the third of (4.4). Predicted volume strains for various distention ratios as a function of applied pressure for the ceramic types P1350 and M1345 are shown in Figures 9 and 10.

The reference values for the specific volumes of the FE and AFE phases were estimated from chemical composition and unit cell dimensions[17] of the FE and AFE phases yielding $\upsilon_{0F} \approx 0.1245\,\text{g/cm}^3$ and $\upsilon_{0A} \approx 0.1238$ g/cm^3. The bulk modulus of the AFE in the solid matrix used in the estimate shown in Figures 9 and 10 was taken $K_A \approx$ 122.3 GPa. An improved estimate of K_A could be obtained from experimental data but is not required for the purpose of this study.

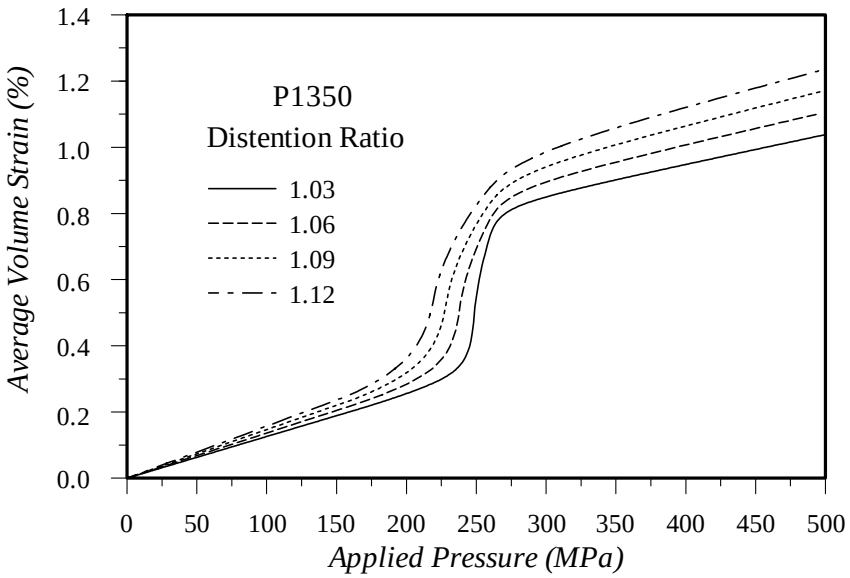

Fig. 9 Model predictions for the average volume strain, including the FE to AFE phase transformation, with increasing applied pressure of porous P1350 ceramic at four different distention ratios.

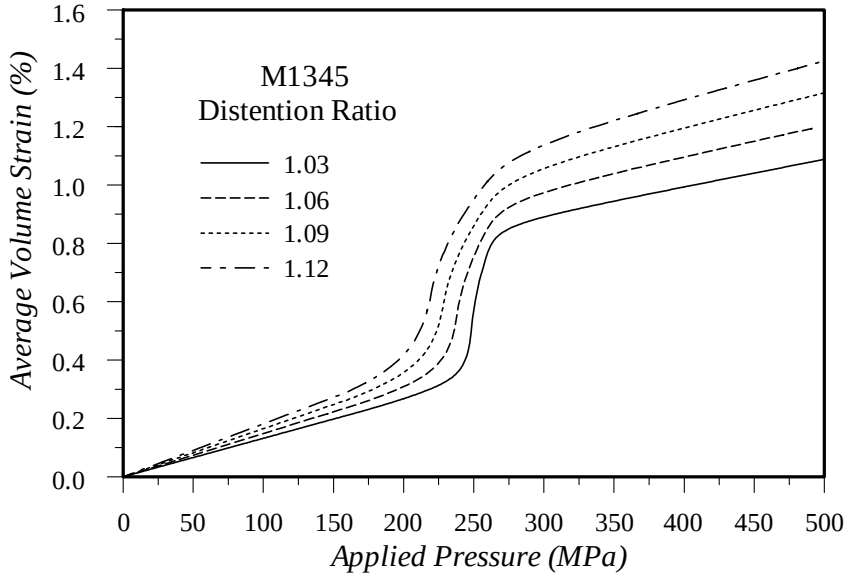

Fig. 10 Model predictions for the average volume strain, including the FE to AFE phase transformation, with increasing applied pressure of porous P1345 ceramic at four different distention ratios.

5. Summary

The effects of porosity and pore morphology on the elastic properties of three types of unpoled PZT 95/5-2Nb have been characterized in this study. It was found possible to characterize each of the three types of ceramic by using four material properties and the porosity. The bulk modulus and shear modulus of solid PZT 95/5-2Nb ceramic, which provide two of the material properties, are common to all three type of porous ceramic examined, and a method of estimating reasonable values for these two properties was described. The other two material properties are different for each ceramic type and reflect effects due to ceramic microstructure. It was seen that pore space morphology produces a significant effect with ceramic material fabricated using PMMA spheres being stiffer than ceramic material fabricated using the rod-like MCC pore former. It was also observed that processing differences effected the elastic properties, even though the ceramics were fabricated using the same pore former. The two ceramics made using the rod-like MCC pore former showed slight differences in elastic properties when processed at different sintering temperatures resulting in similar microstructures characterized by different average ceramic grain sizes. The material with a larger average grain size showed slightly more compliant elastic properties.

The analysis of these ceramic materials was enabled by developing a specific elastic response model for porous material. The model was structured to depend explicitly on the level of porosity, two elastic moduli of the solid PZT 95/5-2Nb ceramic matrix, and two additional parameters that reflect the microstructure of the ceramic. It was found possible to separate the effect of porosity level from the effects of pore morphology and grain size by assuming a specific dependence on porosity level for the two additional parameters, and this observation allowed the elastic response for the three types of unpoled porous PZT 95/5-2Nb to be described by the relations (4.1) and the values listed in Table 3. Based on the observations of this study, it appears that if fabrication of porous PZT 95/5-2Nb ceramic is well controlled, model parameter characterization could be performed at a single porosity value and reliably extrapolated to other values. It would be interesting to investigate other porous materials for a similar characterization.

The elastic response model was shown to provide reasonable estimates for the effective bulk modulus and effective shear modulus values measured for the three types of unpoled porous PZT 95/5-2Nb ceramic characterized indicating consistency of the methodology used in this study.

Finally, a simple extension of the elastic response model was introduced to allow treatment of the FE to AFE phase transformation during hydrostatic pressurization. The volumetric strain predicted using the model reflected observed effects due to changing porosity level and indicated that effects due to microstructural differences should be observable.

References

1. B. Jaffe, W. R. Cook, Jr., and H. Jaffe, *Piezoelectric Ceramics* (Academic, London, 1971).

2. I. J. Fritz and J. D. Keck, J. Phys. Chem. Solids **39**, 1163 (1978).

3. W. J. Halpin, J. Appl. Phys. **37**, 153 (1966).

4. P. C. Lysne and C. M. Percival, J. Appl. Phys. **46**, 1519 (1975).

5. L. J. Storz and R. H. Dungan, Sandia National Laboratories Report, SAND85-1612 (1985).

6. R. H. Dungan and L. J. Storz, J. Am. Ceram. Soc. **68**, 530 (1985).

7. B. A. Tuttle, P. Yang, J. H. Gieske, J. A. Voigt, T. W. Scofield, D. H. Zeuch, and W. R. Olson, J. Am. Ceram. Soc. **84**, 1260 (2001).

8. D. H. Zeuch, S. T. Montgomery, L. W. Carlson, and J. M. Grazier, Sandia National Laboratories report, SAND1999-0635 (1999).

9. P. Yang, R. H. Moore, S. J. Lockwood, B. A. Tuttle, J. A. Voigt, and T. W. Scofield, Sandia National Laboratories Report, SAND2003-3866 (2003).

10. S. T. Montgomery and D. H. Zeuch, in *Ceramic Engineering and Science Proceedings (Vol. 25, No. 4)*, edited by E. Lara-Curzio and M. J. Readey (The American Ceramic Society, 2004) pp. 313-318.

11. R. Hill, J. Mech. Phys. Solids **11**, 357 (1963).

12. A. J. M. Spencer, *Continuum Mechanics* (Longman, London and New York, 1980).

13. M. Carroll and A. C. Holt, J. Appl. Phys. **43**, 759 (1972).

14. J. D. Eshelby, Proc. Roy. Soc. (London) **A241**, 376 (1957).

15. J. K. MacKenzie, Proc. Phy. Soc. **B63**, 2 (1950).

16. D. H. Zeuch, S. T. Montgomery, and D. J. Holcomb, J. Mater. Res. **15**, 689 (2000).

17. L. C. Chhabildas, M. J. Carr, S. C. Kunz, and B. Morosin, in *Shock Waves in Condensed Matter*, edited by Y. M. Gupta (Plenum, New York, 1986) pp. 785-790.

Appendix A. Formulation of an Elastic Response Model for Porous Ceramic

A model for the elastic response of discretely reinforced composite solids developed by Hill[11] is used to represent the response of porous ceramic materials in this study. Development of the response model is reviewed here using the assumptions that there is a uniform isotropic distribution of elastic reinforcing particles in a uniform elastic matrix and then specialized to a form suitable to a porous solid by replacing the particles with empty space. The review of model development is also provided for completeness, since Hill's description was set forth in a general context with many details used in the present study omitted.

Equilibrium Elastic Responses of Discretely Reinforced Composites

The model expresses the average macroscopic elastic response of the composite in terms of the volume fraction of the inclusions and the average elastic response of inclusion and matrix phases. The concept of representative volume is fundamental to defining the macroscopic fields and properties appropriate to the composite. A representative volume contains enough of the matrix and inclusions to be structurally typical of the composite, so that when uniform surface tractions and displacements are applied to the surface of the volume, the apparent elastic constants obtained from averages of stresses and strains are independent of the values of the applied traction and displacement. Consequently, while the local values of stress and strain may fluctuate rapidly in the space occupied by the constituent phases, a well defined mean value for each exists and contributions from the surface irregularities are negligible. The average values of a quantity are defined as the integral of the quantity over a region corresponding to a representative volume divided by the volume of the region.

The matrix and inclusion phases are taken as isotropic linear elastic solids, and the bulk modulus K and shear modulus G are taken as the fundamental pair of elastic constants characterizing each material. The elastic constants for the matrix phase will be designated using the subscript '1' and those for the inclusion phase using the subscript '2'. Elastic constants without a subscript, as above, will refer to the macroscopic averages for the composite. Tensor suffix notation[12] is used to denote the components of the stress (σ_{ij}) and strain (ε_{ij}) tensors. The stress and strain in the matrix phase will be designated using the superscripts '(1)' and by '(2)' for the inclusion phase. The relations between stress and strain in the constituent materials are therefore

$$\sigma_{ij}^{(1)} = \left(K_1 - \frac{2}{3} G_1 \right) \varepsilon_{kk}^{(1)} \delta_{ij} + 2 G_1 \varepsilon_{ij}^{(1)} \quad \text{and} \quad \sigma_{ij}^{(2)} = \left(K_2 - \frac{2}{3} G_2 \right) \varepsilon_{kk}^{(2)} \delta_{ij} + 2 G_2 \varepsilon_{ij}^{(2)} . \qquad \text{(A.1)}$$

It is evident from the definitions above that the average values of the stress and strain in a representative volume are

$$\tilde{\sigma}_{ij} = c_1 \tilde{\sigma}_{ij}^{(1)} + c_2 \tilde{\sigma}_{ij}^{(2)} \quad \text{and} \quad \tilde{\varepsilon}_{ij} = c_1 \tilde{\varepsilon}_{ij}^{(1)} + c_2 \tilde{\varepsilon}_{ij}^{(2)} \qquad \text{(A.2)}$$

where c_1 is the fraction of the representative volume containing the matrix phase, c_2 is the fraction of the representative volume containing the inclusion phase, and the tilde symbol over a quantity indicates that it is an average of the quantity over the representative volume. The assumption of perfect bonding between the inclusions and matrix gives the following constraint between volume fractions of matrix and inclusion phases

$$c_1 + c_2 = 1 . \qquad \text{(A.3)}$$

Consequently, (A.2) may be alternately written

$$\tilde{\sigma}_{ij} = \tilde{\sigma}_{ij}^{(1)} + c_2 \left[\tilde{\sigma}_{ij}^{(2)} - \tilde{\sigma}_{ij}^{(1)} \right] \quad \text{and} \quad \tilde{\varepsilon}_{ij} = \tilde{\varepsilon}_{ij}^{(1)} + c_2 \left[\tilde{\varepsilon}_{ij}^{(2)} - \tilde{\varepsilon}_{ij}^{(1)} \right] . \qquad \text{(A.4)}$$

Because the distribution of individual phases in the representative volume of the composite are uniform and isotropic, the stress-strain relations given by (A.1) hold for the averages in each phase giving, *i.e.*,

$$\tilde{\sigma}_{ij}^{(1)} = \left(K_1 - \frac{2}{3} G_1 \right) \tilde{\varepsilon}_{kk}^{(1)} \delta_{ij} + 2 G_1 \tilde{\varepsilon}_{ij}^{(1)} \quad \text{and} \quad \tilde{\sigma}_{ij}^{(2)} = \left(K_2 - \frac{2}{3} G_2 \right) \tilde{\varepsilon}_{kk}^{(2)} \delta_{ij} + 2 G_2 \tilde{\varepsilon}_{ij}^{(2)} . \qquad \text{(A.5)}$$

Composite materials comprised of isotropic elastic constituents are not necessarily also isotropic. For example, a composite material might be constructed with a regular cubic array of inclusions so that the macroscopic response of a representative volume would be expected to have the symmetry of a cubic crystal. Here it is assumed that the matrix contains a uniform isotropic distribution of inclusions so that the expected response of a representative volume of the composite is isotropic. The relation between the apparent stress and strain of a representative volume will then be

$$\tilde{\sigma}_{ij} = \left(K - \frac{2}{3} G \right) \tilde{\varepsilon}_{kk} \delta_{ij} + 2 G \tilde{\varepsilon}_{ij} . \qquad \text{(A.6)}$$

Equations (A.4) and (A.5) provide relations between average field quantities in the composite but require additional information relating average field quantities before they can be used to represent the elastic response of the composite in terms of the volume fraction of the inclusions

and elastic properties of the matrix and inclusion phases. Suppose that for the range of loadings of interest the average strains in the matrix and inclusion phase are uniquely related to the average strain for the representative volume according to

$$\tilde{\varepsilon}_{ij}^{(1)} = A_{ijkl}^{(1)}\,\tilde{\varepsilon}_{kl} \quad \text{and} \quad \tilde{\varepsilon}_{ij}^{(2)} = A_{ijkl}^{(2)}\,\tilde{\varepsilon}_{kl}\,. \tag{A.7}$$

The tensors $A_{ijkl}^{(1)}$ and $A_{ijkl}^{(2)}$ reflect characteristics of the composite since they will depend on the volume concentrations and microstructure of matrix and inclusions. Substituting (A.7) into the second of (A.2) provides a specific constraint between the components of $A_{ijkl}^{(1)}$ and $A_{ijkl}^{(2)}$:

$$c_1\,A_{ijkl}^{(1)} + c_2\,A_{ijkl}^{(2)} = \delta_{ik}\,\delta_{jl}\,. \tag{A.8}$$

Presuming that the transformations between average strains given by (A.7) maintain isotropy of the composite implies that both $A_{ijkl}^{(1)}$ and $A_{ijkl}^{(2)}$ are fourth-order isotropic tensors, and since $\tilde{\varepsilon}_{ij} = \tilde{\varepsilon}_{ji}$, the simplest representations for $A_{ijkl}^{(1)}$ and $A_{ijkl}^{(2)}$ allowed that maintains isotropy[12] are

$$A_{ijkl}^{(1)} = \left(\kappa_1 - \frac{2}{3}\gamma_1\right)\delta_{ij}\,\delta_{kl} + 2\,\gamma_1\,\delta_{ik}\,\delta_{jl} \quad \text{and} \quad A_{ijkl}^{(2)} = \left(\kappa_2 - \frac{2}{3}\gamma_2\right)\delta_{ij}\,\delta_{kl} + 2\,\gamma_2\,\delta_{ik}\,\delta_{jl}\,. \tag{A.9}$$

The parameters κ_1, κ_2, γ_1, and γ_2 will depend on volume concentrations and microstructure of matrix and inclusions, and provide parameters for characterization of the composite in addition to the elastic properties of the constituent materials. Substituting (A.9) into (A.7) gives

$$\tilde{\varepsilon}_{ij}^{(1)} = \left(\kappa_1 - \frac{2}{3}\gamma_1\right)\tilde{\varepsilon}_{kk}\,\delta_{ij} + 2\,\gamma_1\,\tilde{\varepsilon}_{ij} \quad \text{and} \quad \tilde{\varepsilon}_{ij}^{(2)} = \left(\kappa_2 - \frac{2}{3}\gamma_2\right)\tilde{\varepsilon}_{kk}\,\delta_{ij} + 2\,\gamma_2\,\tilde{\varepsilon}_{ij}\,. \tag{A.10}$$

The constraint of (A.8) then yields

$$c_1\,\kappa_1 + c_2\,\kappa_2 = \frac{1}{3} \quad \text{and} \quad c_1\,\gamma_1 + c_2\,\gamma_2 = \frac{1}{2}\,, \tag{A.11}$$

and implies that only one of the parameter sets (κ_1, κ_2) and (γ_1, γ_2) is independent. Selecting the parameter pair (κ_1, γ_1) as independent gives

$$\kappa_2 = \frac{1 - 3c_1\,\kappa_1}{3c_2} \quad \text{and} \quad \gamma_2 = \frac{1 - 2\,c_1\,\gamma_1}{2\,c_2}\,. \tag{A.12}$$

Since the average strain in the matrix and composite must be the same when there are no inclusions in the composite, (A.3) and (A.11) imply that $3\kappa_1 = 1$ and $2\gamma_1 = 1$ when $c_2 = 0$.

Equations (A.4), (A.5), (A.10) and (A.12) provide a complete description for the average elastic response of the composite once the average strain in the composite as follows:

$$
\begin{aligned}
\tilde{\sigma}_{ij} &= \tilde{\sigma}_{ij}^{(1)} + c_2\left[\tilde{\sigma}_{ij}^{(2)} - \tilde{\sigma}_{ij}^{(1)}\right] \\
\tilde{\sigma}_{ij}^{(1)} &= \left(K_1 - \frac{2}{3}G_1\right)\tilde{\varepsilon}_{kk}^{(1)}\,\delta_{ij} + 2G_1\,\tilde{\varepsilon}_{ij}^{(1)} \\
\tilde{\sigma}_{ij}^{(2)} &= \left(K_2 - \frac{2}{3}G_2\right)\tilde{\varepsilon}_{kk}^{(2)}\,\delta_{ij} + 2G_2\,\tilde{\varepsilon}_{ij}^{(2)} \\
\tilde{\varepsilon}_{ij}^{(1)} &= \left(\kappa_1 - \frac{2}{3}\gamma_1\right)\tilde{\varepsilon}_{kk}\,\delta_{ij} + 2\gamma_1\,\tilde{\varepsilon}_{ij} \\
\tilde{\varepsilon}_{ij}^{(2)} &= \left(\kappa_2 - \frac{2}{3}\gamma_2\right)\tilde{\varepsilon}_{kk}\,\delta_{ij} + 2\gamma_2\,\tilde{\varepsilon}_{ij} \\
\kappa_2 &= \frac{1-3\left(1-c_2\right)\kappa_1}{3c_2} \\
\gamma_2 &= \frac{1-2\left(1-c_2\right)\gamma_1}{2c_2}
\end{aligned}
\tag{A.13}
$$

In addition to the volume fraction of the inclusions, six parameters are needed to use (A.13) to determine the elastic response of the composite. The four parameters K_1, G_1, K_2, and G_2 are the elastic properties of the inclusion and matrix phases and, consequently, may be determined independent of the composite. The two remaining parameters κ_1 and γ_1 relate the average strain in the composite to the average strain in the matrix and, consequently, must reflect effects of the composition and microstructure on the elastic response.

The effective elastic properties of the composite material may be used to determine the parameters κ_1 and γ_1 needed in the response model above. Expressions for the effective elastic properties of the composite may be obtained by substituting (A.5) with (A.10) into the first of (A.2) yielding

$$
\tilde{\sigma}_{ij} = \left\{3\left(c_1\kappa_1 K_1 + c_2\kappa_2 K_2\right) - \frac{4}{3}\left(c_1\gamma_1 G_1 + c_2\gamma_2 G_2\right)\right\}\tilde{\varepsilon}_{kk}\,\delta_{ij} + 4\left(c_1\gamma_1 G_1 + c_2\gamma_2 G_2\right)\tilde{\varepsilon}_{ij}\,. \tag{A.14}
$$

Comparison of (A.6) and (A.14) yields the following correspondence between the effective elastic properties for the composite and the parameters appearing in the elastic response model

$$
K = 3\left(c_1\kappa_1 K_1 + c_2\kappa_2 K_2\right), \quad G = 2\left(c_1\gamma_1 G_1 + c_2\gamma_2 G_2\right). \tag{A.15}
$$

Using the constraints of (A.3) and (A.11) in (A.15) yields

$$K = K_2 + 3\left(1-c_2\right)\kappa_1\left(K_1 - K_2\right) \quad \text{and} \quad G = G_2 + 2\left(1-c_2\right)\gamma_1\left(G_1 - G_2\right) . \qquad \text{(A.16)}$$

Equilibrium Elastic Responses of Porous Ceramics

The elastic response model for the discretely reinforced composite material can be used to describe the equilibrium elastic response of porous ceramic by letting the stiffness of the inclusion phase vanish. Changing the superscript "1" to "S" to indicate the solid ceramic of the matrix and letting the stiffness of the inclusion phase vanish, the equations for the average stress and strain in the porous ceramic and matrix and solid matrix become

$$\begin{aligned} \tilde{\sigma}_{ij} &= \left(1-\varphi\right)\tilde{\sigma}^S_{ij} \\ \tilde{\sigma}^S_{ij} &= \left(K_S - \frac{2}{3}G_S\right)\tilde{\varepsilon}^S_{kk}\,\delta_{ij} + 2G_S\,\tilde{\varepsilon}^S_{ij} \\ \tilde{\varepsilon}^S_{ij} &= \left(\kappa_S - \frac{2}{3}\gamma_S\right)\tilde{\varepsilon}_{kk}\,\delta_{ij} + 2\gamma_S\,\tilde{\varepsilon}_{ij} \end{aligned} \qquad \text{(A.17)}$$

Expressions for the average stress and strain in the pore space are not required. Because the average strain in the matrix and porous ceramic must be the same in the limit of vanishing porosity the last of (A.17) implies that as $\varphi \to 0$, $\kappa_S \to 1/3$ and $\gamma_S \to 1/2$. From (A.16), it is clear that the parameters κ_S and γ_S can be determined from the effective elastic moduli of the porous ceramic using

$$K = 3\left(1-\varphi\right)\,\kappa_S\,K_S \quad \text{and} \quad G = 2\left(1-\varphi\right)\,\gamma_S\,G_S . \qquad \text{(A.18)}$$

Distribution

1	MS 0346	R. S. Chambers, 1524
1	0346	S. T. Montgomery, 1524
1	0346	M. A. Neidigk, 1524
1	0346	E. D. Reedy, 1526
1	0372	E. Corona, 1524
1	0372	J. F. Dempsey, 1524
1	0372	J. Pott, 1524
1	0372	W. M. Sherzinger, 1524
1	0847	P. J. Wilson, 1520
1	0862	T. A. Haverlock, 2734
1	0862	S. C. Hwang, 2734
1	0862	L. A. Paz, 2734
1	0869	E. G. Bujewski, 2715
1	0871	R. A. Damerow, 2730
1	0878	M. O. Eatough, 2735
1	0878	T. W. Scofield, 2735
1	1159	S. C. Jones, 1344
1	1195	J. L. Wise, 1646
1	1245	C. B. Diantonio, 2454
1	1245	S. J. Lockwood, 2454
1	1245	R. H. Moore, 2454
1	1245	A. W. Roesler, 2454
1	1245	P. Yang, 2454
1	1322	J. B. Aidun, 1435
1	1322	J. Robins, 1435
1	1411	B. A. Tuttle, 1816
1	MS 0899	Technical Library, 9536 (electronic copy)